Article

Impact of Solid-State Charge Injection on Spectral Photoresponse of NiO/Ga2O3 P-N Heterojunction

Alfons Schulte , Sushrut Modak , Yander Landa , Atman Atman , Jian-Sian Li , Chao-Ching Chiang , Fan Ren , Stephen J Pearton , Leonid Chernyak *

Posted Date: 30 October 2023

doi: 10.20944/preprints202310.1814.v1

Keywords: Gallium Oxide; spectral photoresponse; minority carriers

Article

Impact of Solid-State Charge Injection on Spectral Photoresponse of NiO/Ga_2O_3 p-n Heterojunction

Alfons Schulte [1,4,*], Sushrut Modak [1], Yander Landa [1], Atman Atman [1], Jian-Sian Li [2], Chao-Ching Chiang [2], Fan Ren [2], Stephen J. Pearton [3] and Leonid Chernyak [1,*]

[1] Department of Physics, University of Central Florida, Orlando, FL 32816, USA
[2] Department of Chemical Engineering, University of Florida, Gainesville, FL 32611, USA
[3] Material Science and Engineering, University of Florida, Gainesville, FL 32611, USA
[4] College of Optics and Photonics, University of Central Florida, Orlando, FL 32816, USA
* Correspondence: alfons.schulte@ucf.edu; leonid.chernyak@ucf.edu

Abstract: Forward-bias hole injection from 10 nm-thick p-type Nickel Oxide layers into 10 mm-thick n-type Gallium Oxide in a vertical NiO/Ga_2O_3 p-n heterojunction leads to more than a factor of 2 enhancement of photoresponse measured from this junction. While it takes only 600 seconds to obtain such a pronounced increase in photoresponse, it persists for hours, indicating feasibility of photovoltaic device performance control. The effect is ascribed to charge injection-induced increase of minority carrier (hole) diffusion length (resulting in improved collection of photogenerated non-equilibrium carriers) in n-type b-Ga_2O_3 epitaxial layers, due to trapping of injected charge (holes) on deep meta-stable levels in the material and subsequent blocking of non-equilibrium carrier recombination through these levels. Suppressed recombination leads to increased non-equilibrium carrier lifetime, in turn determining a longer diffusion length and being the root-cause for the effect of charge injection.

Keywords: Gallium Oxide; spectral photoresponse; minority carriers

I. Introduction

Solar-blind photodetectors [1–4] are insensitive to infrared, visible, and near-UV light, but respond to ultraviolet radiation with wavelengths below about 300 nm. These detectors are critical for a variety of applications, including:

- Flame detection: Solar-blind photodetectors can be used to detect flames, which emit UV light, even in the presence of sunlight or other visible light sources. This makes them useful for fire safety applications, such as in industrial plants and aircraft.
- Missile launch detection: Solar-blind photodetectors can be used to detect missile launches, which also emit UV light. This makes them useful for military and security applications.
- Astronomical observation: Solar-blind photodetectors can be used to observe astronomical objects in the UV spectrum, which is not possible with traditional optical telescopes.
- Ozone layer monitoring: Solar-blind photodetectors can be used to monitor the ozone layer, which absorbs UV light. This information can be used to track the depletion of the ozone layer and to predict the effects of climate change.

Solar-blind photo-devices are typically made from semiconductors with a wide band gap. This means that only high-energy UV photons can be absorbed and generate a photocurrent.

 doi:10.20944/preprints202310.1814.v1

Modern aircrafts need to be equipped with warning sensors operating in the ultraviolet (UV) part of the spectrum, especially in the Ultraviolet-C (UVC) region spanning from 200 to 280 nm wavelength, because the UVC is completely absorbed by the atmospheric ozone layer and, therefore, only a UVC source of interest in the atmosphere below the ozone layer can be detected with solar blind sensors [1–4]. The low false-alarm rate of the UV sensors is due to absence of background radiation, especially in the UVC region.

An emerging semiconductor with a direct bandgap of 4.6-4.9 eV, β-Ga_2O_3 has become an attractive candidate for sensing applications in UVC region primarily due to its ultra-wide bandgap and superior radiation stability (due to wider bandgap) over GaN [1–8]. A drawback with Ga_2O_3 is the absence of robust p-type doping. All the potential acceptor dopants have large ionization energies and are not significantly ionized at room temperature. This has led to the use of p-type oxides, principally polycrystalline NiO, to form p-n heterojunctions with n-type Ga_2O_3 [9–17]. The forward current transport mechanism in such junctions is typically recombination under low bias and trap-assisted tunneling under higher bias [13,19–24]. Conductivity modulation has been demonstrated during switching in these heterojunctions [25].

It has been previously shown that in p-type GaN and ZnO, electron beam or solid-state injection, using forward bias of p-n junctions, results in a significant increase of the minority carrier diffusion length [24,26–28]. Similar effects have been recently observed in n-type and highly resistive p-type Ga_2O_3 subjected to low energy electron beam injection in Scanning Electron Microscopes [29,30]. Diffusion length increase translates into experimentally demonstrated superior photovoltaic detector performance for GaN [31] and ZnO [32,33], with evidence of a similar effect for β-Ga_2O_3. However, the effect of electrical injection of carriers has not been demonstrated in this material because of the lack of p-type doping capability.

This work demonstrates the impact of forward bias charge injection on photoresponse in NiO/Ga_2O_3 p-n heterojunctions at room temperature. The results, which are summarized below, present the proof of concept and pave the road towards device performance control in Ga_2O_3 solar-blind UV photodetectors.

II. Experimental

The schematic for the vertical p-n NiO/Ga_2O_3 heterojunction is shown in Figure 1. The epitaxial layers were grown by Halide Vapor Phase Epitaxy (HVPE) on a (001) Sn-doped ($2x10^{18}$ cm^{-3}) β-Ga_2O_3 single crystal substrate. These samples were purchased from Novel Crystal Technology, Japan [34]. They consisted of a lightly doped drift layer on a conducting substrate. The drift region thickness was 10 μm, grown by halide vapor phase epitaxy (HVPE) on a (001) Sn-doped (10^{19} cm^{-3}) β-Ga_2O_3 single crystal substrate. The NiO bilayer was deposited by rf (13.56 MHz) magnetron sputtering at a working pressure of 3 mTorr [17,35]. The NiO bilayer consisted of 20 nm layer, with hole concentration p = 10^{18} cm^{-3}, and 10 nm layer, with hole concentration p = $2.6x10^{19}$ cm^{-3}, which were optimized to provide high breakdown voltage and optimal current spreading, respectively. The hole concentration in the NiO bilayer was adjusted using the Ar/O_2 ratio. The structure was then annealed at 300 °C under O_2. Finally, a top contact of 20/80 nm Ni/Au (1000 μm diameter) was deposited onto the NiO bilayer. Ohmic contacts were made to the rear surface using a Ti/Au metal stack deposited by e-beam evaporation followed by annealing at 550 °C for 180 s under N_2. The front surface was subjected to UV/Ozone exposure for 15 minutes to remove contamination prior to the metal deposition. More details on the vertical p-n NiO/Ga_2O_3 heterojunction fabrication can be found elsewhere [35].

 doi:10.20944/preprints202310.1814.v1

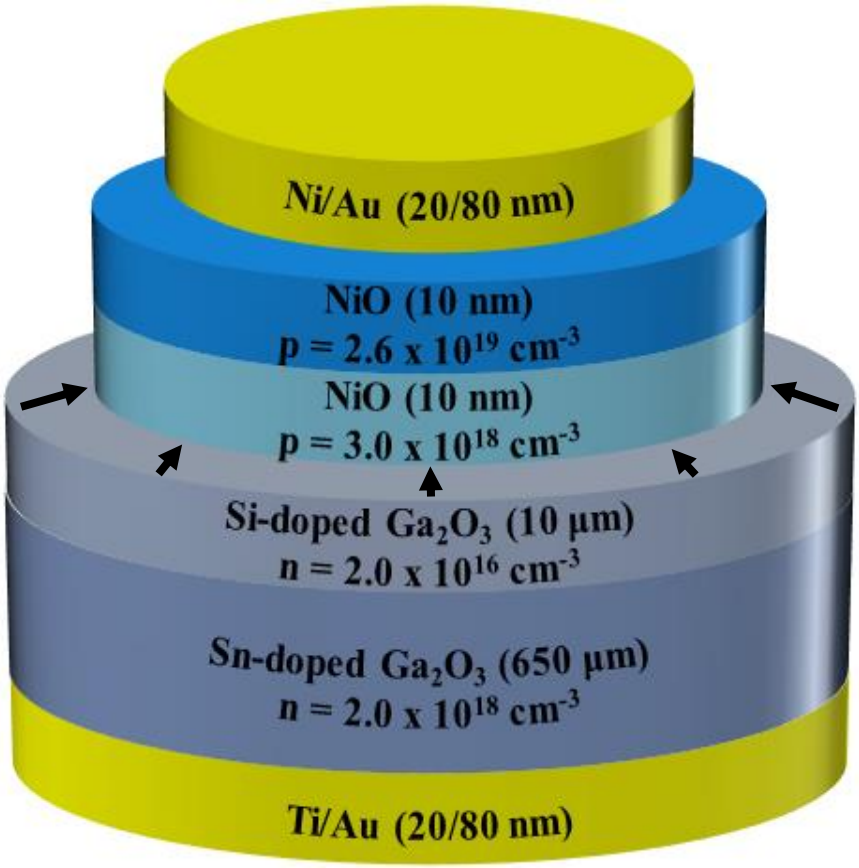

Figure 1. Schematics for the vertical p-n NiO/Ga_2O_3 heterojunction with the respective majority carrier concentrations and thicknesses. The centripetal arrows on the top plane of Si-doped 10 mm-thick n-type Ga_2O_3 layer show directions for a lateral diffusion and drift of light-induced non-equilibrium minority holes moving towards the space-charge region, which extends by ~ 180 nm beyond the p-NiO/n-Ga_2O_3 interface.

The heterojunction shows the rectification of more than 5 orders of magnitude from 2V forward to 10 V reverse bias, as shown in Figure 2a,b. The forward turn-on voltage for the junction is ~ 1.9 V (cf. Figure 2b) with on-resistance of 8 $m\Omega.cm^{-2}$ [35]. Under forward bias, the depletion layer is collapsed, and holes diffuse into the Ga_2O_3. Drift is the dominating carrier transport under reverse bias due to the electric field. Diffusion is more important in the neutral region. There is a slight (0.2 V) offset in the I-V curve, due to residual charges on the diode [36]. The I-V curve in this case shows a slightly different offset when the voltage swings from different directions.

 doi:10.20944/preprints202310.1814.v1

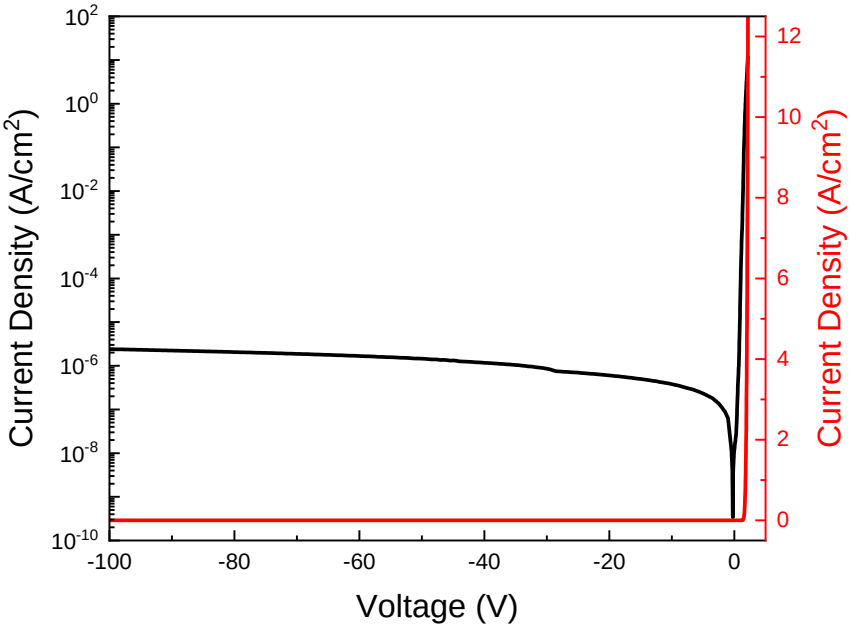

(a)

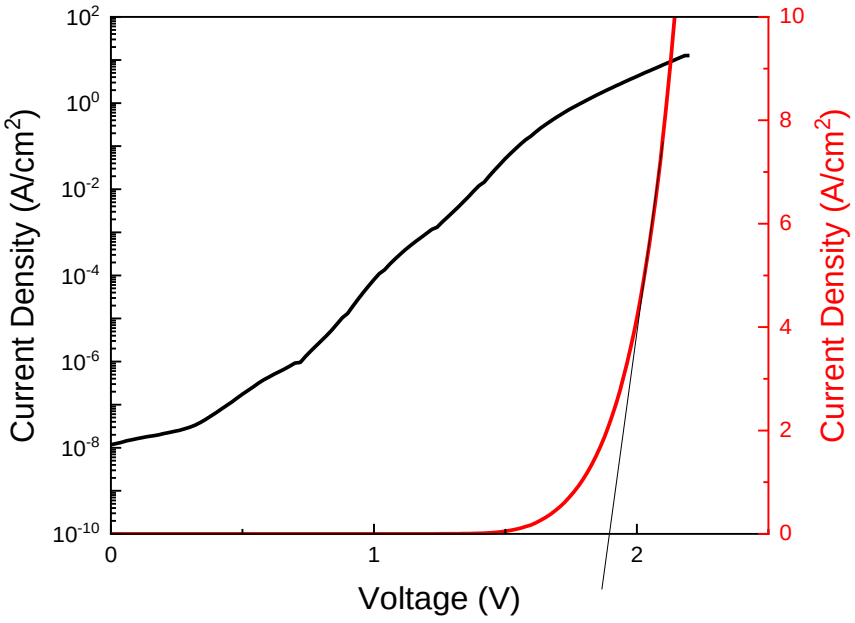

(b)

Figure 2. (a): Room temperature forward and reverse I-V curves (linear and logarithmic scales) from NiO/Ga_2O_3 p-n heterojunction shown in Figure 1. **(b):** Forward branch of the I-V curve shown in Figure 2, a (linear and logarithmic scale). The value for forward turn-on voltage of ~ 1.9 V is obtained by intersection of dashed line, tangential to the I-V curve, with Voltage axis.

The dominant carrier transport mechanism in the heterojunction diodes (HJDs) is trap-assisted tunneling [36]. Because the doping level for p-NiO layer in Figure 1 is two orders of magnitude larger as compared to that of n-Ga_2O_3, the heterojunction can be treated as a one-sided abrupt junction. Therefore, the lateral and vertical extension, d, of the depletion layer at p^+-NiO/n-Ga_2O_3 interface can be calculated as $d = [2ee_0(V_{bi}-V)/(qN_B)]^{0.5}$, where e_0 stands for permittivity in vacuum; e is Ga_2O_3 dielectric constant; V_{bi} – built-in potential; V – applied external bias; q – charge of electron; N_B – bulk

 doi:10.20944/preprints202310.1814.v1

10 mm-thick n-type Sn:Ga_2O_3 doping level (cf. Figure 1). Using the values presented for a similar calculation in ref. [29], resulted in d ~ 180 nm under zero bias. The maximum electric field strength at p-NiO/n-Ga_2O_3 interface was estimated at 0.8 MV.cm^{-1}, well below the maximum breakdown field of ~8 MV.cm^{-1} [37].

The I-V curves of p^+-NiO/n-Ga_2O_3 heterojunction, presented in Figure 2a,b, were measured using a Keithley 2400 Source Meter. The measurements were carried out at room temperature. The same instrument was employed to drive a forward current of 100 mA through the structure in Figure 1 for the total duration of 900 seconds, corresponding to the maximum charge of 90 mC. The forward current resulted in charge injection from p-NiO to n-Ga_2O_3 layers and led to the results presented in the following section of this paper.

Room temperature spectral photoresponse was measured under zero bias in the 200-300 nm spectral range using a tunable light source, comprising a stabilized deuterium UV lamp (SLS204) coupled with Horiba Triax 320 spectrometer. The latter is equipped with a grating having 2400 grooves/mm blazed at 250 nm. The output beam of monochromatic light was focused in the shape of a rectangle (fully covering the whole top contact and extending to the opposite sides of it; cf. Figure 1) and modulated at 95 Hz frequency. The induced photoresponse signal, measured at zero-bias, was amplified using an Ithaco 393 lock-in amplifier, digitized with a Keithley 2000 digital multimeter, and recorded using a homemade software. The spectra were recorded prior to forward bias charge injection, followed by recording after 300, 600 and 900 seconds of bias.

III. Results and discussion

The room temperature photoresponse from the structure in Figure 1 is presented in Figure 3 as a function of forward bias duration. All spectra exhibit shoulders at about 255 nm, corresponding to the direct band-to-band transition in b-Gallium Oxide [1–3,38]. The maxima for all spectra are observed between 230 and 240 nm and likely correspond to the excitonic absorption. Similar photoresponse peaks were recently observed between 5.0 and 5.2 eV (238-248 nm wavelength range) in ref. [39], consistent with the band structure of the monoclinic Ga_2O_3 [38].

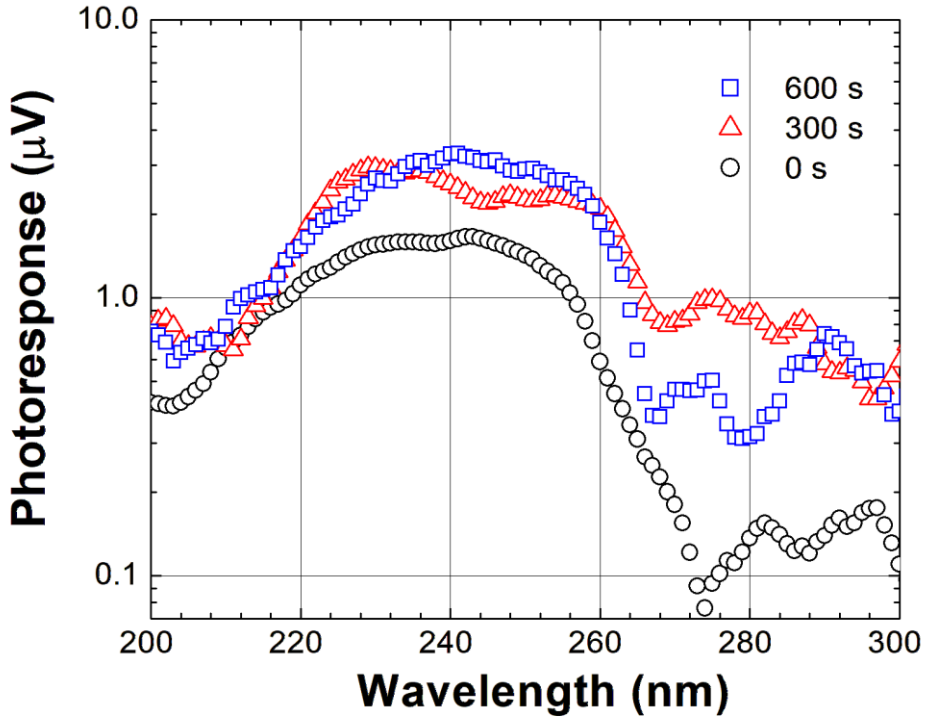

Figure 3. Spectral photoresponse (in log scale) under zero bias for the vertical p-n NiO/Ga_2O_3 heterojunction in Figure 1 as a function of forward-bias hole injection duration. 100 mA was driven for the total duration of 600 seconds.

 doi:10.20944/preprints202310.1814.v1

An increase of more than a factor of 2 in peak photoresponse was observed in Figure 3 while injecting the total charge of 60 mC for 600 seconds. Forward bias was continued for the total time of 900 seconds; however, the pick photo-signal didn't show an additional increase, thus indicating saturation for the effect of interest.

Ref. [29] reports detailed studies of charge injection-induced effects in n-type b-Ga_2O_3 subjected to low-energy (10 kV) electron beam irradiation *in-situ* in a Scanning Electron Microscope (SEM), which resulted in x4 increase of minority carrier (holes) diffusion length in the material at room temperature. Elongation of the diffusion length (L), measured using Electron Beam-Induced Current (EBIC) technique in the region of charge-injection, was accompanied by a simultaneous decrease of cathodoluminescence (CL) intensity from the same region, which confirms suppression of radiative recombination with increasing duration of charge injection. Because L is proportional to the square root of non-equilibrium carrier lifetime, t, and CL intensity is proportional to t^{-1}, both effects (L elongation and CL intensity decrease) were attributed to a lifetime increase of non-equilibrium carriers in the conduction and valence bands. Variable temperature EBIC measurements revealed a charge trap with the activation energy of 74 meV, which was responsible for the phenomena under investigation.

The experimental results, observed in Figure 3 of this article, as well as previously obtained results for GaN and ZnO structures [24,26,28,32,33], suggest the following:

1. Charge injection from the electron beam of SEM and forward-bias injection, reported in this work, demonstrate similarities in terms of their impact on minority carrier diffusion length in Gallium Oxide. As was already mentioned above, forward bias application to NiO/Ga_2O_3 p-n junction results in a decrease of the potential barrier (~ 1.03 V for V_{bi}) at the interface of two semiconducting layers [29]. As a result, the holes from p-NiO are injected into n-Ga_2O_3 and, likely, get captured by meta-stable traps. Although the exact energetic location for these possible traps is yet unknown, ref. [36] recently reported a trapping level for holes in n-type Ga_2O_3 located 140 meV above the top of the valence. This level was revealed by Deep Level Transient Spectroscopy (DLTS) technique while studying hole injection via trap-assisted tunneling from p^+-NiO into n-Ga_2O_3 under forward bias. Capturing injected charge carriers on the meta-stable energetic levels, prevents recombination of light-induced non-equilibrium carriers in n-type Gallium Oxide through these levels. As a result, the non-equilibrium carriers remain in the respective valence and conduction bands of Gallium Oxide for longer times, in turn leading to larger carrier lifetime, t, and, therefore, longer diffusion length, L.

2. Although L was not directly measured for the structure, shown in Figure 1 and studied in the experiments reported here, it is logical to assume that forward bias charge injection leads to an increase of minority hole diffusion length in the 10 mm-thick n-type Ga_2O_3 epitaxial layer in agreement with the mechanism described above and in ref. [29]. Because the concentration of majority carriers in n-Ga_2O_3 is two orders of magnitude lower, as compared to that in p-NiO, the built-in electric field, employed for non-equilibrium carrier charge separation, is mostly localized in the 10 mm-thick n-type Gallium Oxide epitaxial layer (extends ~ 180 nm from the NiO/Ga_2O_3 interface into 10 mm-thick n-Gallium Oxide [29]). Therefore, the diffusion length for minority holes in this layer are of primary importance.

3. According to ref. [41], which studied absorption of UV radiation (at 250 nm) in NiO/Ga_2O_3 heterojunction, more than 80% of the light, shining vertically on the Ni/Au/NiO stack (cf. Figure 1), is absorbed and, therefore, doesn't reach the underlying 10 mm-thick n-type Gallium Oxide epitaxial layer. As a result, the only portion of 10 mm-thick Si-doped n-Ga_2O_3, which is not covered by the above Ni/Au contact and NiO bilayer, contributes to the photoresponse. Therefore, the collection of non-equilibrium photoexcited carriers in n-Ga_2O_3 is lateral, as shown by the centripetal arrows in Figure 1, meaning that the non-equilibrium minority carriers are mostly swept by the vertical portion of the NiO/Ga_2O_3 space charge region, which extends laterally (~ 180 nm) beyond the heterojunction interface.

4. Minority hole diffusion length, L, measured at room temperature in ref. [29] for n-type Ga_2O_3 using Electron Beam-Induced Current (EBIC) technique, was reported at ~ 400 nm prior to electron beam injection. It is generally accepted that light-excited (due to illumination) non-equilibrium

 doi:10.20944/preprints202310.1814.v1

carriers, generated within 2L distance from the space-charge region, are capable of diffusing without recombination towards the p-n junction, where they are swept by its internal electric field, thus contributing to a photocurrent. Therefore, longer diffusion length, due to forward-bias charge injection, leads to collection of photogenerated carriers from a larger area of the structure presented in Figure 1, thus enhancing collection (by the p-n heterojunction built-in field) efficiency for minority carriers (holes), and, therefore, representing the main factor, which contributes to larger photoresponse with increasing duration of forward bias [39].

5. It should be noted that the structure in Figure 1 is not optimized as a photo-detecting device. Therefore, instead of presenting device's figures of merit, the relative photoresponse increase is demonstrated in Figure 3, thus serving as the proof of concept.

The dynamics of photoresponse increase as a function of forward bias duration is presented in Figure 4. The peak photoresponse exhibits a linear increase as a function of time (injected charge) before it saturates (not shown in the figure). The nature of linear increase is related to two factors:

1. Minority carrier diffusion length depends linearly on injection duration (charge) as was previously observed for Gan, ZnO, and Ga_2O_3 [24,28,29].

2. In the configuration of the structure under test, in which the charge collection occurs laterally (cf. Figure 1 and the discussion outlined above), the photoresponse depends linearly on L, as seen in Figure 4 and as explained in ref. [42].

The inset of Figure 4 demonstrates relaxation of the photoresponse under polychromatic illumination followed saturation (cf. Figure 3 and the above discussion). It is critical to emphasize that while it takes only 600 seconds to induce a more than a factor of 2 increase in the peak photoresponse, it takes much longer time (up to 6000 seconds) for the signal to decay to the baseline. This serves as a proof for the metastable nature of traps involved in the phenomenon of charge injection.

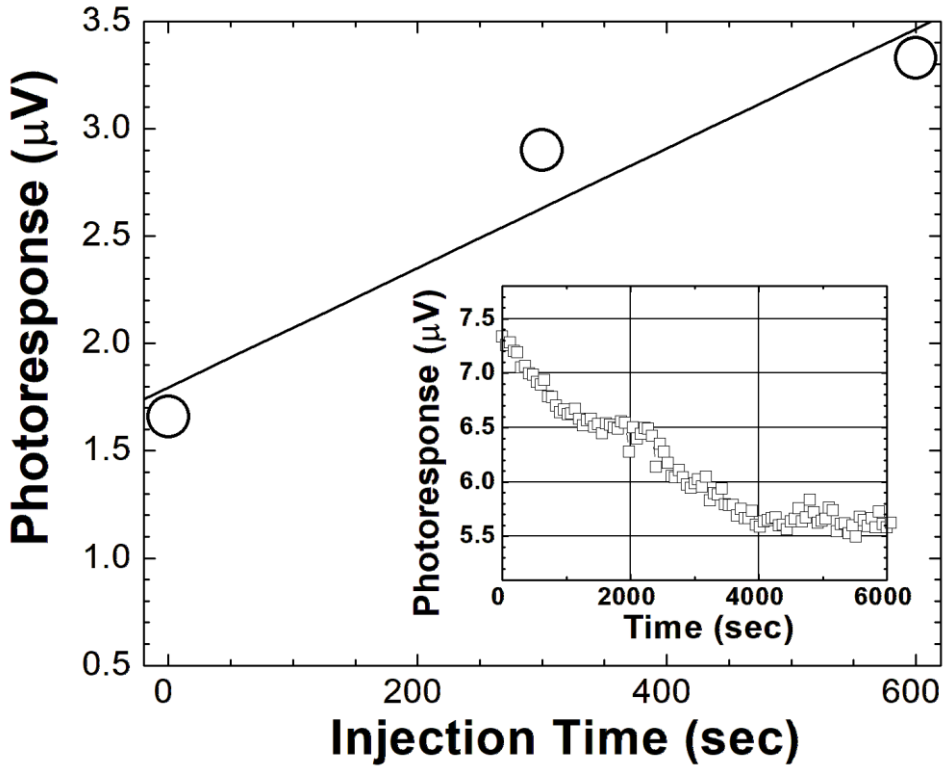

Figure 4. Dynamics for photoresponse enhancement (open circles) and the fit to the data. A saturation trend is observed beyond 600 seconds and is not shown on the graph. The linear fit confirms lateral charge collection as discussed in ref. [42]. **Inset:** Dynamics of polychromatic photoresponse relaxation after 600 seconds of forward bias injection.

IV. Summary

In summary, the effect of charge injection under forward bias was employed for improvement of the photoresponse from the NiO/β-Ga_2O_3 p-n heterojunction. Charging of metastable point defect levels in β-Ga_2O_3 is believed to be responsible for the phenomenon of interest. Because it only takes seconds to induce an enhanced photoresponse and its slow decay occurs over hours, the effect has practical implications for enhancement of detector performance. Combined with electronic circuitry for photosignal monitoring and periodic charge injection, once necessary, a new generation of higher efficiency photovoltaic devices could be fabricated. The advantage of the proposed method is that it does not involve costly technological modifications of the structure but is a purely electrical "athermal" approach, based on defect engineering.

Author Contributions: Conceptualization, L.C.; methodology, S.M., A.S.; software, A.S.; validation, L.C., S.M.; formal analysis, A.S., L.C., S.M.; investigation, Y.L., A.A., J.-S.L., C.-C.C.; writing – original draft preparation, L.C., J.-S.L.; writing – review and editing, L.C., S.J.P.; supervision, A.S., L.C. F.R., S.J.P.; project administration, A.S., L.C., F.R., S.J.P.; funding acquisition, A.S., L.C., F.R., S.J.P. All authors have read and agreed to the published version of the manuscript.

Funding: This research was supported in part by the US-Israel Binational Science Foundation (award # 2022056), the National Science Foundation (ECCS #2310285), and NATO (G5748). The research at UF was performed as part of the Interaction of Ionizing Radiation with Matter University Research Alliance (IIRM-URA), sponsored by the Department of the Defense, Defense Threat Reduction Agency under the award HDTRA1-20-2-0002. The content of the information does not necessarily reflect the position or the policy of the federal government, and no official endorsement should be inferred.

Data Availability Statement: The data presented in this review are openly available from the articles cited in this review paper as well as from the corresponding author upon request.

Conflicts of Interest: The authors declare no conflict of interest.

References

1. Kalra, A.; Ul Muazzam, U.; Muralidharan, R.; Raghavan, S.; Nath, D.N. The road ahead for ultrawide bandgap solar-blind UV photodetectors. *J. Appl. Phys.* **2022**, *131*, 150901.
2. Xie, C.; Lu, X.T.; Tong, X.W.; Zhang, Z.X.; Liang, F.X.; Liang, L.; Luo, L.B.; Wu, Y.C. Recent progress in solar-blind deep-ultraviolet photodetectors based on inorganic ultrawide bandgap semiconductors. *Adv. Funct. Mater.* **2019**, *29*, 1806006.
3. Kaur, D.; Kumar, M. A Strategic Review on Gallium Oxide Based Deep-Ultraviolet Photodetectors: Recent Progress and Future Prospects. *Adv. Opt. Mater.* 2021, **9**, 2002160.
4. Xu, J.; Zheng, W.; Huang, F. Gallium oxide solar-blind ultraviolet photodetectors: a review. *J. Mater. Chem., C*, **2019**, *7*, 8753.
5. Flack, T.J.; Pushpakaran, B.N.; Bayne, S.B. GaN technology for power electronic applications: a review. *J. Electron. Mater.* **2016**, *45*, 2673.
6. Ionascut-Nedelcescu, A.; Carlone, C.; Houdayer, A.; von Bardeleben, H.J.; Cantin, J.-L.; Raymond, S. Radiation hardness of gallium nitride. *IEEE Trans. Nuc. Sci.* **2002**, *49*, 2733.
7. Onoda, S.; Hasuike, A.; Nabeshima, Y.; Sasaki, H.; Yajima, K.; Sato, S.I.; Ohshima, T. Enhanced charge collection by single ion strike in AlGaN/GaN HEMTs. *IEEE Trans. Nuc. Sci.* **2013**, *60*, 4446.
8. Nakamura, S.; Mukai, T.; Senoh, M. High-power GaN pn junction blue-light-emitting diodes. *Jap. J. Appl. Phys.* **1991**, *30*, L1998.
9. Kokubun, Y.; Kubo, S.; Nakagomi, S. All-oxide p–n heterojunction diodes comprising p-type NiO and n-type β-Ga_2O_3. *Appl. Phys. Express* **2016**, *9*, 091101.
10. Deng, Y.; Yang, Z.; Xu, T.; Jiang, H.; Ng, K.W.; Liao, C.; Su, D.; Pei, Y.; Chen, Z.; Wang, G.; Lu, X. Band alignment and electrical properties of NiO/β-Ga_2O_3 heterojunctions with different β-Ga_2O_3 orientations. *Appl. Surf. Sci.* **2023**, *622*, 156917.
11. Pintor-Monroy, M.I.; Barrera, D.; Murillo-Borjas, B.L.; Ochoa-Estrella, F.J.; Hsu JW, P.; Quevedo-Lopez, M.A. Tunable Electrical and Optical Properties of Nickel Oxide (NiO_x) Thin Films for Fully Transparent NiO_x–Ga_2O_3 p–n Junction Diodes. *ACS Appl. Mater. Interfaces* **2018**, *10*, 38159.
12. Xia, X.; Li, J.-S.; Chiang, C.-C.; Yoo, T.J.; Ren, F.; Kim, H.; Pearton, S.J. Annealing temperature dependence of band alignment of NiO/β-Ga_2O_3. *J. Phys. D: Appl. Phys.* **2022**, *55*, 385105.
13. Gong, H.; Chen, X.; Xu, Y.; Chen, Y.; Ren, F.; Liu, B.; Gu, S.; Zhang, R.; Ye, J. Band Alignment and Interface Recombination in NiO/β-Ga_2O_3 Type-II pn Heterojunctions. *IEEE Trans. Electron. Dev.* **2020**, *67*, 3341.

14. Sharma, S.; Zeng, K.; Saha, S.; Singisetti, U. Field-Plated Lateral Ga2O3 MOSFETs With Polymer Passivation and 8.03 kV Breakdown Voltage. *IEEE Electron. Dev. Lett.* **2020**, *41*, 836.
15. Zhang, J.; Dong, P.; Dang, K.; Zhang, Y.; Yan, Q.; Xiang, H.; Su, J.; Liu, Z.; Si, M.; Gao, J.; Kong, M.; Zhou, H.; Hao, Y. Ultra-wide bandgap semiconductor Ga_2O_3 power diodes. *Nat. Commun.* **2022**, *13*, 3900.
16. Dong, P.; Zhang, J.; Yan, Q.; Liu, Z.; Ma, P.; Zhou, H.; Hao, Y. 6 kV/3.4 mΩ·cm² Vertical β-Ga_2O_3 Schottky Barrier Diode With $BV^2/R_{on,sp}$ Performance Exceeding 1-D Unipolar Limit of GaN and SiC. *IEEE Electron. Dev. Lett.* **2022**, *43*, 765.
17. Li, J.-S.; Chiang, C.-C.; Xia, X.; Yoo, T.J.; Ren, F.; Kim, H.; Pearton, S.J. Demonstration of 4.7 kV breakdown voltage in NiO/β-Ga_2O_3 vertical rectifiers. *Appl. Phys. Lett.***2022**, *121*, 042105.
18. Lv, Y.; Wang, Y.; Fu, X.; Dun, S.; Sun, Z.; Liu, H.; Zhou, X.; Song, X.; Dang, K.; Liang, S.; Zhang, J.; Zhou, H.; Feng, Z.; Cai, S.; Hao, Y. Demonstration of β-Ga_2O_3 Junction Barrier Schottky Diodes With a Baliga's Figure of Merit of 0.85 GW/cm² or a 5A/700 V Handling Capabilities. *IEEE Trans. Power Electr.* **2021**, *36*, 6179.
19. Liao, C.; Lu, X.; Xu, T.; Fang, P.; Deng, Y.; Luo, H.; Wu, Z.; Chen, Z.; Liang, J.; Pei, Y.; Wang, G. Optimization of NiO/β-Ga_2O_3 Heterojunction Diodes for High-Power Application. *IEEE Trans. Electron. Dev.* **2022**, *69*, 5722.
20. Xiao, M.; Wang, B.; Liu, J.; Zhang, R.; Zhang, Z.; Ding, C.; Lu, S.; Sasaki, K.; Lu, G.-Q.; Buttay, C.; Zhang, Y. Packaged Ga_2O_3 Schottky Rectifiers With Over 60-A Surge Current Capability. *IEEE Trans. Power Electr.* **2021**, *36*, 8565.
21. Lu, X.; Zhou, X.; Jiang, H.; Ng, K.W.; Chen, Z.; Pei, Y.; Lau, K.M.; Wang, G. 1-kV Sputtered p-NiO/n-Ga_2O_3 Heterojunction Diodes With an Ultra-Low Leakage Current Below 1 μA/cm². *IEEE Electron. Dev. Lett.* **2020**, *41*, 449.
22. Wang, C.; Gong, H.; Lei, W.; Cai, Y.; Hu, Z.; Xu, S.; Liu, Z.; Feng, Q.; Zhou, H.; Ye, J.; Zhang, J.; Zhang, R.; Hao, Y. Demonstration of the p-NiO_x/n-Ga_2O_3 Heterojunction Gate FETs and Diodes With $BV^2/R_{on,sp}$ Figures of Merit of 0.39 GW/cm² and 1.38 GW/cm². *IEEE Electron. Dev. Lett.* **2021**, *42*, 485.
23. Yan, Q.; Gong, H.; Zhang, J.; Ye, J.; Zhou, H.; Liu, Z.; Xu, S.; Wang, C.; Hu, Z.; Feng, Q.; Ning, J.; Zhang, C.; Ma, P.; Zhang, R.; Hao, Y. β-Ga_2O_3 hetero-junction barrier Schottky diode with reverse leakage current modulation and BV2/Ron, sp value of 0.93 GW/cm². *Appl. Phys. Lett.* **2021**, *118*, 122102.
24. Chernyak, L.; Osinsky, A.; Fuflyigin, V.; Schubert, E.F. Electron beam-induced increase of electron diffusion length in p-type GaN and AlGaN/GaN superlattices. *Appl. Phys. Lett.* **2000**, *77*, 875.
25. Zhou, F.; Gong, H.; Xiao, M.; Ma, Y.; Wang, Z.; Yu, X.; Li, L.; Fu, L.; Tan, H.H.; Yang, Y.; et al. An avalanche-and-surge robust ultrawide-bandgap heterojunction for power electronics. *Nat. Commun.* **2023**, *14*, 4459.
26. Chernyak, L.; Osinsky, A.; Schulte, A. Minority carrier transport in GaN and related materials. *Solid-State Electron.* **2001**, *45*, 1687.
27. Chernyak, L.; Nootz, G.; Osinsky, A. Enhancement of minority carrier transport in forward biased GaN pn junction. *Electron. Lett.* **2001**, *37*, 922.
28. Lopatiuk-Tirpak, O.; Chernyak, L.; Xiu, F.X.; Liu, J.L.; Jang, S.; Ren, F.; Pearton, S.J.; Gartsman, K.; Feldman, Y.; Osinsky, A.; Chow, P. Studies of minority carrier diffusion length increase in p-type ZnO:Sb. *J. Appl. Phys.* **2006**, *100*, 086101.
29. Modak, S.; Lee, J.; Chernyak, L.; Yang, J.; Ren, F.; Pearton, S.J.; Khodorov, S.; Lubomirsky, I. Electron injection-induced effects in Si-doped β-Ga_2O_3. *AIP Advances* **2019**, *9*, 015127.
30. Modak, S.; Schulte, A.; Sartel, C.; Sallet, V.; Dumont, Y.; Chikoidze, E.; Xia, X.; Ren, F.; Pearton, S.J.; Ruzin, A.; Chernyak, L. Impact of radiation and electron trapping on minority carrier transport in p-Ga_2O_3. *Appl. Phys. Lett.* **2022**, *120*, 233503.
31. Chernyak, L.; Schulte, A.; Osinsky, A.; Graff, J.; Schubert, E.F. Influence of electron injection on performance of GaN photodetectors. *Appl. Phys. Lett.* **2002**, *80*, 926.
32. Lopatiuk-Tirpak, O.; Chernyak, L.; Mandalapu, L.J.; Yang, Z.; Liu, J.L.; Gartsman, K.; Feldman, Y.; Dashevsky, Z. Influence of electron injection on the photoresponse of ZnO homojunction diodes. *Appl. Phys. Lett.* **2006**, *89*, 142114.
33. Lopatiuk-Tirpak, O.; Nootz, G.; Flitsiyan, E.; Chernyak, L.; Mandalapu, L.J.; Yang, Z.; Liu, J.L.; Gartsman, K.; Osinsky, A. Influence of electron injection on the temporal response of ZnO homojunction photodiodes. *Appl. Phys. Lett.* **2007**, *91*, 042115.
34. Yang, J.; Ren, F.; Chen, Y.-T.; Liao, Y.-T.; Chang, C.-W.; Lin, J.; Tadjer, M.J.; Pearton, S.J.; Kuramata, A. Dynamic Switching Characteristics of 1 A Forward Current β -Ga_2O_3 Rectifiers. *IEEE J. Electron Dev. Society* **2019**, *7*, 57.
35. Li, J.-S.; Xia, X.; Chiang, C.-C.; Hays, D.C.; Gila, B.P.; Craciun, V.; Ren, F.; Pearton, S.J. Deposition of sputtered NiO as a p-type layer for heterojunction diodes with Ga_2O_3. *J. Vac. Sci. Technol. A* **2023**, *41*, 013405.
36. Wang, Z.; Gong, H.; Meng, C.; Yu, X.; Sun, X.; Zhang, C.; Ji, X.; Ren, F.; Gu, S.; Zheng, Y.; Zhang, R.; Ye, J. Majority and Minority Carrier Traps in NiO/β-Ga2O3 p+-n Heterojunction Diode. *IEEE Trans. Electron Devices* **2022**, *69*, 981.

37. Wang, Z.P.; Gong, H.H.; Yu, X.X.; Hu, T.C.; Ji, X.L.; Ren, F.-F.; Gu, S.L.; Zheng, Y.D.; Zhang, R.; Ye, J.D. Traps inhomogeneity induced conversion of Shockley–Read–Hall recombination in NiO/β-Ga_2O_3 p^+–n heterojunction diodes. *Appl. Phys. Lett.* **2023**, *122*, 152102.
38. Furthmüller, J.; Bechstedt, F. Quasiparticle bands and spectra of Ga_2O_3 polymorphs. *Phys. Rev. B*. **2016**, *93*, 115204.
39. Verma, D. Measurement of Local Electric Fields and the Onset of Breakdown in Ultra-wide Band Gap Semiconductor Devices using Photocurrent Spectroscopy. Ph.D. Thesis, Ohio State, 2023.
40. Modak, S.; Chernyak, L.; Schulte, A.; Sartel, C.; Sallet, V.; Dumont, Y.; Chikoidze, E.; Xia, X.; Ren, F.; Pearton, S.J.; Ruzin, A.; Zhigunov, D.M.; Kosolobov, S.S.; Drachev, V.P. Variable temperature probing of minority carrier transport and optical properties in p-Ga_2O_3. *APL Materials* 2022 **10**, 031106.
41. Vasquez JM, T.; Ashai, A.; Lu, Y.; Khandelwal, V.; Rajbhar, M.; Kumar, M.; Li, X.; Sarkar, B. A self-powered and broadband UV PIN photodiode employing a NiO_x layer and a β-Ga_2O_3 heterojunction. *J. Phys. D: Appl. Phys.* **2023**, *56*, 065104.
42. Holloway, H. Theory of lateral-collection photodiodes. *J. Appl. Phys.* **1978**, *49*, 4264,.